Biosorption of Azure Dye with Sunflower Seed Hull: Estimation of Equilibrium, Thermodynamic and Kinetic Parameters

Gbekeloluwa Oguntimein[1] , James Hunter[2] and Dong Hee Kang[3]

Department of Civil Engineering, Morgan State University,5200 Perring Parkway Baltimore MD 21251,USA

Abstract:-Biosorption potential of sunflower seed hull to remove reactive textile dye contaminated solutions was the purpose of this investigation. Azure A chloride dye was chosen as a model for this investigation. Pretreatment, initial pH, biomass dosage, contact time, initial dye concentration and temperature were evaluated in batch mode studies. Preliminary results indicate that acid and base pretreatment affected the dye biosorption properties of the milled hull. Particles retained on the ASTM sieves 250 μm and 425 μm had the highest biosorption capacity. The optimum pH for azure dye biosorption was 6.0, and the values of percent dye biosorbed and biosorption capacity increased with contact time and dosage of dried sunflower seed hull (DSSH). Batch equilibrium data obtained at different temperatures (22.5, 25, 30, 35, 35, 40 and 45°C) were modeled by Freundlich, Langmuir and Dubinin–Radushkevich (D–R) isotherms. Langmuir and Freudlich isotherms model fitted the equilibrium data, at all studied temperatures. The highest monolayer biosorption capacity was found to be 22.27mg g^{-1} dry biomass at 40°C. The changes in Gibbs free energy (ΔG^{*}), enthalpy (ΔH^{*}) and entropy (ΔS^{*}) of biosorption were also evaluated for the biosorption of Azure dye onto DSSH. The results indicate that the biosorption was spontaneous and exothermic. The kinetic properties were studied; the data fitted the first and pseudo second order model at room temperature (22.5^{o}C). The pseudo-second-order kinetic model was observed to provide the best correlation of the experimental data among the kinetic models studied. The biosorbent–dye interaction mechanisms were investigated using Fourier transform infrared spectroscopy.

Keywords:- Biosorption, Azure dye, pseudo-second order kinetics, Isotherms, dried sunflower seed hull

I.   INTRODUCTION

The contamination of the industrial waters with the organic based chemicals has created a serious environmental problem. Synthetic dyes, one group of organic pollutants, are extensively used in several industries such as textile, paper, printing and dye houses. The effluents from these industries are highly colored and discharge of dye containing effluents into the natural water bodies can pose hazardous effects on the living systems because of carcinogenic, mutagenic, allergenic and toxic nature of dyes. The presence of very small amounts of dyes in water (less than 1 mg dm^{-3} for some dyes) is highly visible and undesirable. The conventional decolorization methods of dye bearing wastewaters involve the combination of physical and chemical processes such as precipitation, sedimentation, ultrafiltration, flotation, color irradiation, ozonation and coagulation. However the application of the above mentioned technologies is sometimes restricted due to technical and economic constraints. Also synthetic dyes have a complex aromatic molecular structure, which makes them stable and resistant to biological degradation .Adsorption is an effective alternative process for the treatment of contaminated wastewater. Currently, activated carbon is the most popular and extensively used commercial biosorbent material due to its high adsorption capacity, surface area and degree of surface reactivity as well as micro porous structures. But it shows some disadvantages such as high operating costs and regeneration problems [1]. Therefore, in the recent years considerable amount of researches have been done on the development of effective, low cost and easily available alternative biosorbents. Different agricultural biomasses such as tree fern [2], peat and rice husk [3,4], peanut hull [5,6], sugarcane dust [7] , apple pomace and wheat straw [8,9] , bark [10], palm kernel fibre [11], banana peel and orange peel [12,13] , coir pith [14] , linseed cake [15] and sawdust [16-18] have been previously tried for the removal of different types of dyes, but high effective and more economical biosorbent materials are still needed.

The sunflower plant is a native of North America. It was grown by the Indians for food in North Carolina before 1600 and by New England colonists for hair oil as early as 1615 [19]. The rising prominence of sunflower oil in world edible oil markets has stimulated increased interest in expanded U.S production for last decades. U.S acreage of sunflower planting has expanded rapidly in the 1970's, reaching a peak at 5.5 million acres. The U.S sunflower production has declined in recent years. Currently U.S planted sunflower over 1.8 million arcres in 2012 and approximately 1 million metric tons of sunflower seed were produced in 2011. 41% and 32.7 % of total sunflower planted acres were grown in the North Dakota and South Dakota in 2012,

respectively [20] . Compared with soybean oil which currently dominates the US edible oils market, sunflower seed oil has a higher content of polyunsaturated fatty acids [19].

The world production of sunflower seed is 31.1 MT with the USSR being the largest producer producing 6.3MT, Ukraine 4.7MT, Argentina 3.7MT , China 1.9MT, India 1.9MT, USA 1.8MT [21]. The U.S produced around 6% of the world's sunflower production and 85.1 % of total U.S sunflower production is for vegetable oils. In recent years, approximately 12 million acres of sunflowers have been grown in the world annually [22] . The hull accounts for 22 to 28% of the weight of sunflower seed and becomes a byproduct of the seed crushing operation. Large-seed varieties have higher proportion of hull than small-seed varieties. The most promising use for sunflower seed hulls appears to be as roughage ingredient for livestock feed. Sunflower hulls make coarse roughage, high in fiber but suitable for use in ruminant rations. Sunflower hull contains11.5% moisture, 3.5% protein 3.4% fat, and 22.1 % fiber [19] .

The objectives of this study were to investigate the potential use of sunflower seed hull, as an effective biosorbent for the removal of dye from aqueous solutions and study its thermodynamic and kinetic properties. There has been no reported study to date in this field on the use of sunflower seed hull as a biosorbent.

II.   MATERIAL and METHODS

II.1 *Preparation of Sunflower seed Hull (SSH)*

A 120g packet of Sunflower seeds purchased from a local grocery was dehulled and the hull was milled in a coffee grinder. The milled hull was then separated into different particle seizes using with ASTM standard sieves with mesh seizes 60 (250μm aperture), 40 (425μm aperture) and 20 (850μm aperture). The fraction of the sunflower seed which is hull was determined by dehulling a known weight of seed and weighing the hull separated.

The effect of acid and base treatment was studied using the fraction retained on the 40 mesh sieve. Three grams each of milled hull was soaked overnight in either 250 mL of 0.05M hydrochloric acid (HCl) or 250mL of 0.05M sodium hydroxide (NaOH). The pHs of the supernatants were 1.4 and 12.7 respectively. The supernatant was removed and each fraction was washed thrice with 250 mL distilled water (dH$_2$O). The pH of the acid treated sunflower seed hull (SSH) was then adjusted to pH 5.0 with drops of 1M NaOH while the base treated SSH was adjusted to pH 5.5 with drops of 1 M HCl. The wet SSH was dried overnight at 70°C in a forced air drying oven to constant weight. The dried sunflower seed hull (DSSH) was used in the adsorption characteristics studies.

II.2 *Preparation of Azure Dye solution*

Azure dye (C$_{14}$H$_{14}$N$_3$SCl; MW 291.5 g mol^{-1}) shown in figure 1 was obtained from Sigma Co., St Louis, MO. The dye showed a maximum absorbance at wavelength 600 nm. Stock dye solution (1 mM) was prepared by dissolving 291.5mg of Azure dye in dH$_2$O and other concentrations were prepared by dilution of the stock solution. All the chemicals used in this study were in analytical grade.

II.3 *Dye biosorption experiments*

Batch biosorption experiments were performed in 50 mL plastic tubes containing 20 mLdye solution with vortex mixing. Aliquot of 1mL were withdrawn every 15min for absorbance measurement at 600nm using a GENESYS 5 Scanning Spectrophotometer (Thermo Scientific, Madison, WI , USA) to determine the concentration of dye. The concentration of azure dye was determined from a calibration plot of absorbance at 600nm versus concentration. The calibration plot was linear up to an Azure dye concentration of 1mM. In order to determine the effective biosorption conditions, experiments were conducted with both acid and based treated SSH, different particle seizes SSH, at different pH values, and initial dye concentrations. To determine the effect of concentration of azure dye on adsorption capacity, 0.2g of DSSH was weighed into the 50mL plastic tubes and 10 mL solution of 0.05 M acetate buffer pH 6.0 to each tube followed by 10 mL of different concentrations (0.05-0.1mM) of Azure dye   stock solutions. To determine the effect of initial pH on biosorption characteristics of DSSH,0.2 g of DSSH was weighed into 50 mL plastic tubes and 20 mL of 0.1mM solution of Azure dye solution whose pH had been adjusted with different concentrations of HCL and NaOH. To determine the effect of particle size of DSSH on adsorption of azure dye, 0.5 g of DSSH of different particle seizes (<250μm, 250 μm -425 μm , 425 μm -850 μm ,>850 μm) was weighed into 50 mL plastic tubes and to each tube was added 20 mL of 0.05 mM solution of Azure dye and vortex mixed every ten minutes. All experiments were conducted at room temperature 22.5 ^{o}C in triplicates. The amount of Azure dye biosorbed per gram of DSSH was calculated using the following equation (1):

$$q = [C_o - C_t] * \frac{V}{M}$$ ……………………………………………………………………… (1)

Where q is the biosorption of Azure dye per gram of DSSH(mg g^{-1}); C$_o$ is the initial concentration of Azure dye (mg L^{-1}) and C$_t$ is the concentration at time t (mg L^{-1}); V is the total volume of the suspension (L); M is the dry weight (mass) of DSSH (g). The percent dye biosorbed (PDB) from aqueous solution by DSSH was calculated using equation (2) :

$$PDB = \left[1 - \frac{C_o}{C_t} \right] * 100\% \dots\dots\dots\dots\dots\dots\dots\dots\dots\dots\dots\dots\dots\dots\dots\dots\dots\dots\dots \text{(2)}$$

Where C$_t$ is the Azure dye concentration (mg L^{-1}) at time t and C$_o$ is the initial dye concentration (mg L^{-1})

II.3. Kinetic modeling

The kinetics of Azure dye biosorption on DSSH was analyzed using three kinetic models: the pseudo-first order and pseudo second order and intraparticle diffusion model [6,23]. The pseudo first order kinetics equation is generally expressed as:

$$\frac{dq_t}{dt} = k_1 [q_e - q_t] \dots\dots\dots\dots\dots\dots\dots\dots\dots\dots\dots\dots\dots\dots\dots\dots\dots\dots\dots \text{(3)}$$

where q$_e$ is the biosorption capacity of Azure dye on DSSH at equilibrium determined from experimental data (mg g^{-1}); q$_t$ is the biosorption capacity of Azure dye by DSSH at a particular time (mg g^{-1}); k$_1$ is the pseudo-first order rate constant (g mg^{-1} min^{-1}). After integration and applying boundary conditions t=0 and t=t, the integrated form of equation (3) becomes

$$Ln[q_e - q_t] = Lnq_e - k_1 t \dots\dots\dots\dots\dots\dots\dots\dots\dots\dots\dots\dots\dots\dots\dots\dots\dots\dots \text{(4)}$$

From the plot of Ln(q$_e$ - q$_t$) versus time (t), k$_1$ and q$_e$ can be determined from the slope and intercept respectively. The pseudo second-order kinetics equation is expressed as

$$\frac{dq_e}{dt} = k_2 [q_e - q_t]^2 \dots\dots\dots\dots\dots\dots\dots\dots\dots\dots\dots\dots\dots\dots\dots\dots\dots\dots \text{(5)}$$

where q$_e$ is the biosorption capacity of Azure dye by DSSH at equilibrium determined from experimental data (mg g^{-1}); q$_t$ is the biosorption capacity of Azure dye by DSSH at a particular time (mg g^{-1}); k$_2$ is the pseudo-second order rate constant (mg g^{-1} min^{-1}). After integration and applying boundary conditions t=0 and t=t, the integrated form of equation (5) becomes

$$\frac{1}{[q_e - q_t]} = \frac{1}{q_e} + k_2 t \dots\dots\dots\dots\dots\dots\dots\dots\dots\dots\dots\dots\dots\dots\dots\dots\dots \text{(6)}$$

Equation (6) can be rearranged to obtain a linear form

$$\frac{t}{q_t} = \frac{1}{k_2 q_e^2} + \frac{t}{q_e} \dots\dots\dots\dots\dots\dots\dots\dots\dots\dots\dots\dots\dots\dots\dots\dots\dots\dots \text{(7)}$$

where h (mg g^{-1}min^{-1}) can be regarded as the initial sorption rate as q$_t$ t^{-1} , hence

$$h = k_2 q_e^2 \dots\dots\dots\dots\dots\dots\dots\dots\dots\dots\dots\dots\dots\dots\dots\dots\dots\dots\dots\dots\dots \text{(8)}$$

Equation. (7) then becomes

$$\frac{t}{q_t} = \frac{1}{h_e} + \frac{t}{q_e} \dots\dots\dots\dots\dots\dots\dots\dots\dots\dots\dots\dots\dots\dots\dots\dots\dots\dots\dots \text{(9)}$$

If the pseudo-second order kinetics is applicable to the experimental data, the plot of t q$_t$$^{-1}$ versus t of equation (9) should give a straight line, from which q$_e$ and k$_2$ (the rate constant) can be determined from the slope and intercept of the plot. The results are also analyzed in terms of intraparticle diffusion model to investigate whether the intraparticle diffusion is the rate controlling step in biosorption of Azure dye onto DSSH biomass. The intraparticle diffusion equation is expressed as:

$$q_t = K_{id} t^{0.5} + c \dots\dots\dots\dots\dots\dots\dots\dots\dots\dots\dots\dots\dots\dots\dots\dots\dots\dots\dots \text{(10)}$$

where K$_{id}$ is the intraparticle diffusion rate constant (mg g^{-1} min$^{-0.5}$) and C is the intercept.
Statistical analyses (regression relationship, t-test for significance of slope and intercept values, and t-test for average values) were performed using Microsoft Excel 2007.

III.   RESULT and DISCUSSION

III.1 Effect of treatment on biosorption capacity of DSSH

Figure 2 shows a plot of the biosorption capacity of DSSH after 120 minute incubation. Both the acid and base treated DSSH had a higher biosorption capacity than the non-treated DSSH. Both the acid and base treated DSSH were statistically different(P<0.05) from the non-treated DSSH. Though, the base treated DSSH

(P=0.08) was not significantly different (P>0.05) from the acid treated DSSH, the base treated DSSH had a slightly higher biosorption capacity than the acid treated DSSH. Similar results were obtained with wheat straw by Wang et al. 2012. According to these authors [9], because in the surface of wheat straw, there is large amount of SiO_2 and non-aromatic esters. However, the aqueous NaOH treatment may make esters and SiO_2 dissolved out and then the cellulose, hemicelluloses, and lignin were exposed. Therefore, the more active sites were provided and biosorption specific surface was increased, making for the increase of dye biosorption rate.

III.2 Effect of particle size

The particle size of the biosorbent has a significant influence on the kinetics of adsorption. It furnishes important information of achieving optimum utilization of adsorbent and on the nature of breakthrough curves. Rates of adsorption on a solid surface are expected to vary with available surface area for a contact adsorbent mass with the particle size. The adsorption capacity is directly proportional to the particle diameter for nonporous adsorbents. The presence of a large number of smaller particles provides the adsorption system with a greater surface area available for dye removal [24]. The base treated DSSH was fractionated into different particle sizes and the biosorption capacity of the different sizes were determined. Figure 3 shows the plot of the biosorption capacity after 120 minute incubation. The fraction retained by the 60 mesh seize with particle seize greater than 250µm but less than 425 µm had the highest biosorption capacity and was used in subsequent experiments. The particle size less than 250µm was powdery. Previous studies have also shown that as the particle size decreases the biosorption capacity increases [24,25].

III.3 Effect of time on biosorption

The rate of biosorption is important for designing batch biosorption experiments. Therefore, the effect of contact time on the biosorption of Cu(II) was investigated. In addition the effect of time on adsorption of dye on biomass has been reported in literature [26]. Figure 4 shows the effect of time on PDB which increased considerably until the contact time reached 120 minutes. Further increase in contact time did not enhance the biosorption, so, the optimum contact time was selected as 120 min for further experiments.

III.4. Effect of pH

Previous studies in the literature have shown that solution pH is an important parameter affecting the biosorption process [1,5,27]. Further, pH influences surface properties of the biosorbent by way of functional group dissociation and also surface charges [28] . Figure 5 shows the variation of the biosorption capacity after 120 minutes with different pH values. As the pH increased from 3.5 to 6.0 the biosorption capacity increased after which it decreased at pH 6.5. The PDB on the other hand increased as the pH increased for all pH values. The pH optimum for biosorption of Azure dye by DSSH was around pH 6.0. The maximum dye uptake capacity of DSSH was found to be 2.15mg g^{-1} at a pH value of 6.3. The biosorbent surface has many different functional groups and the net charge on the biosorbent surface is pH-dependent. Therefore, the pH of the medium is an important environmental parameter for dye removal from the aqueous medium [1]. It is well-known that pH can affect protonation of functional groups (i.e. carboxyl, phosphate and amino groups) in the biomass, as well as the chemistry of the dye (i.e. its solubility) [6].

III.4 Effect of Dye concentration

Figure 6 shows the effect of dye concentration on PDB and biosorption capacity at pH 6.0. The maximum PDB occurs at a dye concentration of 20mg L^{-1} while the biosorption capacity (BC) increased linearly with concentration. This was probably due to the increasing driving force in the concentration gradient and increasing electrostatic interactions between surface sites and dye [29]. The linear relationship was fitted to a straight line BC = 0.09C_o with a correlation coefficient of 0.99, where C_o is the initial dye concentration in mg L^{-1}.

III.5 Effect of biomass dosage

The number of sites available for biosorption depends upon the amount of the adsorbent. The increase in the biosorption percentage with increase in biomass dosage is due to increase in active sites on the adsorbent and thus making easier penetration of the dye to the sorption sites [28]. Figure 7 shows the plot of the PDB versus biomass dosage. As it can be seen from this figure, an increase in the biomass concentration from 2.76 to 25.10 g L^{-1} the PDB increased from 47.0 % to 86.0 % after 120 minutes incubation which is the maximum value, whereas the biosorption capacity of the DSSH decreased from 1.27 mg g^{-1} to 0.24 mg g^{-1}. A decrease in the biosorption capacity at higher biomass concentration may be attributed to overlapping or partial aggregation of biosorption sites on the biosorbent surface. This fact results in a decrease in effective surface area of the biosorbent available to the dye[1,27,30] . Further increase in the biosorbent concentration up to 31.0 g L did not significantly change the PDB. This is due to the binding of almost all dye ions to biosorbent surface and the

establishment of equilibrium between the dye molecules on the biosorbent and in the solution [27,31, 32]. Increasing the biosorbent dosage caused an increase in the biomass surface area and in the number of potential binding sites [6].

III.8 Biosorption isotherms

The data obtained from biosorption experiments are generally represented by equilibrium isotherms. These provide more important parameters for designing and optimizing of the biosorption systems. Different isotherm models can be used to determine the biosorption characteristics of a biosorbent. In the present study the Azure dye biosorption was analyzed by three different models Langmuir, Freundlich and Dubinin–Radushkevich (D–R). The data were fitted and the calculated isotherm constants are presented in Table 1. The fundamental assumption of the Langmuir isotherm model is that biosorption takes place at specific sites within the biosorbent. Once a biosorbate occupies a binding site, no further biosorption occurs at this site. In the other words Langmuir model assumes that biosorbed layer is one molecule thickness (monolayer biosorption) [33] .

$$q_e = \frac{q_{max} K_1 C_e}{1 + K_L C_e} \quad \text{..} \quad (11)$$

where q_e is the equilibrium biosorption capacity of Azure dye (mg g^{-1}), C_e is the equilibrium Azure dye concentration in the solution (mg L^{-1}), q_{max} is the monolayer biosorption capacity of the biosorbent (mg L^{-1}), and K_L is the Langmuir constant (L mg^{-1}) and is related to the free energy of biosorption. The linearized form of the Langmuir equation is given below:

$$\frac{1}{q_e} = \frac{1}{q_{max}} + \left(\frac{1_e}{q_{max} K_L}\right)\left(\frac{1}{C_e}\right) \quad \text{...} \quad (12)$$

The effect of isotherm shape has been discussed [34]with a view to predict whether a biosorption system is favorable or unfavorable. The essential feature of the Langmuir isotherm can be expressed by means of 'R$_L$', a dimensionless constant referred to as separation factor or equilibrium parameter. R$_L$ is calculated by using equation (13).

$$R_L = \frac{1}{1 + K_L C_o} \quad \text{...} \quad (13)$$

where C_o is the initial Azure dye concentration (mg L^{-1}). The value of R$_L$ calculated using the above equation is incorporated in Table 1. If the R$_L$ values lie between 0 and 1, the biosorption process is considered to be favorable [34]. Values of K$_L$ and q$_{max}$ are obtained from the intercept and slope of the linear plots at various temperature in Figure 8 and are represented in Table 1. The R$_L$ values obtained in this study were in the range 0.049–0.449, indicating that the biosorption process is favorable. The Freundlich isotherm is an empirical equation assuming that the adsorption process becomes on heterogeneous surfaces and adsorption capacity is related to the concentration of Azure dye at equilibrium. The Freundlich isotherm equation is generally expressed as follows[35] :

$$q_e = K_F C_e^{\frac{1}{n}} \quad \text{...} \quad (14)$$

The linearized form is:

$$Ln q_e = Ln K_F + \frac{1}{n} Ln C_e \quad \text{..} \quad (15)$$

where q_e is the equilibrium Azure dye concentration on the biomass (mg g^{-1}); Ce is the equilibrium dye concentration in the solution (mg L^{-1}); K$_F$ (L mg^{-1}) and n (dimensionless Freundlich isotherm constant being indicative of the extent of the biosorption and the degree of nonlinearity between solution concentration and biosorption, respectively. Values of K$_F$ and n are obtained from the intercept and slope of the linear plots at various temperature in Figure 9 and are represented in Table 1.The numerical values of Freundlich constant of n were between 0.667 and 1.678, which are a measure of the deviation from linearity of the biosorption [30]. They were greater than unity, at 30 and 35°C indicating that Azure dye is favorably adsorbed by DSSH at all these temperatures. The Dubinin–Radushkevich (D–R) isotherm is more general than the Langmuir isotherm since it does not assume a homogeneous surface or constant biosorption potential [36]. The D–R isotherm model describes the biosorption nature of the sorbate on the biosorbent and it is used to calculate the mean free energy of biosorption. The characteristic biosorption curve is related to the porous structure of the biosorbent according to this model. The linearized form of (D–R) equation can be written as:

$$Ln q_e = Ln q_m - \beta \varepsilon^2 \quad \text{..} \quad (16)$$

where q_m is the biosorption capacity of the biosorbent (mg g^{-1}), β is a constant related to the biosorption energy, ε is Polanyi potential which can be presented as:

$$\varepsilon = RTLn *1 + \frac{1}{C_e}$$ ....(17)

where R is the universal gas constant (8.314 J mol^{-1} K^{-1}) and T is the temperature (K). The values of D–R isotherm constants, β and q_m were obtained from the slope and intercept of the linear plot presented in Figure 10. The constant β gives an idea about the mean free energy of biosorption and E value can be computed using the following relationship.

$$E = \frac{1}{\left(2\beta^{\vee}\right)^{0.5}}$$ ....(18)

The magnitude of E value characterize the type of the biosorption as chemical ion exchange (E = 8–16 kJ mol^{-1}) [37], or physical sorption (E<8kJ mol^{-1}) [38]. The mean free energy of biosorption (E) is found between 1.550 and 5.625 kJ mol^{-1} at different temperatures, which implies that, the biosorption of Azure dye on DSSH may be considered as physical biosorption and q_m the theoretical saturation capacity varied between 1.979 and 16.55 mg g^{-1}. According to the correlation coefficient r^2 values in Table I both the Langmuir and Freundlich isotherms model fit the Azure dye biosorption data better than the D-R isotherm model at all studied temperatures.

III.9 Thermodynamic analysis of dye removal process

The equilibrium biosorption capacity of Azure dye onto DSSH was favored at lower temperatures. The thermodynamics constants are presented in Table II. The equilibrium constant increased from 23 to 35°C then decreased as the temperature was increased to 45°C indicating a decrease in the biosorption capacity. In order to determine the temperature dependence of the dye removal process by DSSH, the changes in the thermodynamic parameters (free energy (ΔG^*), enthalpy (ΔH^*) and entropy (ΔS^*)) were analyzed using the Langmuir equilibrium (K_L). The following equations were used to calculate the thermodynamic parameters.

$$\Delta G^* = - RT \ln K_L$$ ....(19)

$$\ln K_L = -\frac{\Delta G^*}{RT} = -\frac{\Delta H^*}{RT} + \frac{\Delta S^*}{R}$$ ....(20)

The Van Hoff plot of $\ln K_L$ as function of $1 * T^{-1}$ from 23 to 35°C is shown in Figure 11 yields a straight line with a correlation coefficient of 0.96 from which ΔH^* and ΔS^* were calculated from the slope and intercept respectively. The negative values of ΔG^* indicate that the biosorption process was spontaneous in nature and confirm the affinity of the biosorbent towards the dye molecules. The negative value of ΔH^* (-128.50 kJ mol^{-1}) suggests the exothermic nature of the biosorption process. The positive entropy value of (519.78 J mol^{-1}) indicates increased randomness at the solid/liquid interface during the biosorption process while low value of ΔS indicates that no remarkable change on entropy occurs [39-41]

III.10 Biosorption kinetics

Biosorption kinetics depends on the sorbate–sorbent interactions and operating conditions. Several kinetic models are available to understand the behavior of the adsorbent and also to examine the controlling mechanism [28]. In this study, the biosorption equilibrium data were analyzed using three kinetic models, pseudo-first-order, pseudo-second-order and intraparticle diffusion model. The kinetic studies were carried out to determine the efficiency of Azure dye adsorption onto DSSH. The biosorption capacity increased with the initial dye concentrations while the PDB had a maximum at a dye concentration of 20 mg L^{-1} Figure 6. From the first pseudo-first order equation (4) [23] values of k_1 calculated from the slope of the plots of from the plot of $\ln(q_e - q_t)$ versus time (t) are given in Table III. It was found that the correlation coefficients for the first-order model are lower than that for the pseudo-second-order model. This implies that the biosorption process does not follow first-order kinetics. For the pseudo-second-order kinetic model equation (7) [23,27] , a plot of $t * q_t^{-1}$ versus t (Figure 12), values of k_2 and q^2 were calculated. These parameters are summarized in Table 3. The calculated q_e values agree with experimental q_e values and the correlation coefficients for the pseudo-second order kinetic plots were very high. These results suggested that the biosorption system studied follows the pseudo-second order kinetic model. Similar results have been observed with peanut hull [6]. The pseudo-second-order rate constants for the biosorption of Azure dye onto DSSH show a steady increase with DSSH dosage. The values of rate constants were found to decrease from 5.96×10^{-2} to 2.34×10^{-2} gm g^{-1} min^{-1} with an increase in biomass dosage from 11.7 to 31.00 mg L^{-1} (Table 3).The values of k_2 the second order rate constant and h the initial biosorption rate were correlated to the initial concentration by the following relationships

$$K_2 = 0.0992\, e^{-0.048C_o}$$

$$H = 0.0459e^{-0.049C_o}$$

The correlation coefficient for these relationships were 0.98 and 0. 93 respectively. Similar relationships were obtained for the biosorption of methylene blue onto palm kernel fibre [42]. Figure 13 shows the plot of q versus the square root of time ($t^{1/2}$). It was observed that all the plots have an initial curved portion, followed by a linear portion and a plateau region. This kind of multi-linearity in the shape of the intraparticle diffusion plot has also been observed in the biosorption of methylene blue by palm kernernel fibre [42]. The three phases in the intraparticle diffusion plot suggest that the sorption process proceeds by surface sorption, intraparticle diffusion and a likely chemical reaction stage. The initial curved portion of the plot indicates a boundary layer effect; the second portion is due to intraparticle diffusion while the third linear portion is likely due to chemical reaction. The initial curve of the plot is due to the diffusion of dye molecule through the solution to the external surface of DSSH biomass. The linear portion of curves describes the gradual biosorption stage, where intraparticle diffusion of dye molecule on DSSH takes place and final plateau region indicates equilibrium uptake. The slope of the second portion of the plot is defined as the intraparticle diffusion parameter K_{id} (mg g^{-1} min $^{-0.5}$). On the other hand, the intercept of the plot reflects the boundary layer effect. The lager the intercept, the greater the contribution of the surface sorption in the rate limiting step. The rate constants of intraparticle diffusion model K_{id} are shown in Table 3. The values increased from 0.06 to 0.24 (mg g^{-1} min $^{-0.5}$) as the concentration increased from 11.73 mg L^{-1} to 28.50 mg L^{-1} then decreased to 0.16(mg g^{-1}min $^{-0.5}$) at 31.00 mg L^{-1}. Based on the results it may be concluded that intraparticle diffusion is not only the rate determining factor [28].

III.11 FTIR analysis

In order to confirm the presence and nature of the binding sites on DSSH and their involvement during biosorption of Azure dye, FTIR studies were carried out. Lignin and cellulose are the main components of agricultural and plant materials. They also include hemicelluloses, extractives, lipids, proteins, simple sugars, starches, water, hydrocarbons, ash and many more compounds. These components have many different functional groups responsible for biosorption processes. The functional groups on the biosorbent surface are the evidence of the presence of some of these components and of responsibility for the biosorption of Azure dye. The FTIR spectra were recorded in the region from 700 to 4000 cm^{-1} for both DSSH ((Fig. 14a) and dye-loaded DSSH biomass (Fig. 14b). There were significant similarities in the spectra before and after biosorption, suggesting that the components and structure of DSSH remained intact. Peak positions were noticed at 3449.2, 2897.84, 1734.68, 1596.33, 1236.13 and 1031.72 cm^{-1}. The bands at 3349.32 are due to O-H and N-H stretching. While the bands at 2897.84 represents the CH$_2$ asymetric stretching vibration. The band at 1596.33 reflect N-H bending [43]. Band at 1236.13 correspond to N-H peptide amide II [44] and band at 1031.72 cm^{-1} correspond to C-O stretching. Compared with the FTIR spectra of the dye loaded DSSH (Fig.14b), the band intensity at 3349.32, 2897.84, 1734.68, 1596.33, 1236.13 and 1031.72 cm^{-1} shifted to 33.42.24, 2938.81, 1735.19, 1589.96 , 1231.85 and 1028.07 cm^{-1} respectively. Additional bands were observed at 1507, and 1415.56 cm^{-1}. Corresponding to N=N groups bending and C-N stretching respectively [43]. The intensity of the bands increased after Azure dye biosorption demonstrating that there was reactions of Azure dye with hydroxyl, amine, N=N groups. The intensities of the peaks at about 2897.84 cm^{-1} on the FTIR spectrum of the dye loaded DSSH biomass, ascribed to –CH$_2$ stretching vibrations were stronger. These findings show possibly involvement of the functional groups on the biosorbent surface in biosorption process.

IV.   CONCLUSION

Biosorption of Azure A chloride dye from aqueous solution by dried milled sunflower seed hull was studied as a function of particle seize, initial pH, initial biomass concentration and acid base treatment. Acid and base treatment affected the dye adsorption properties of the milled hull. Particles retained by sieve >250 μm and < 425 μm had the highest adsorption capacity. The optimum pH for azure dye adsorption was around 6.0. The values of per cent dye biosorbed (PDB) and biosorption capacity (BC) increased with time of contact, dosage of dried sunflower seed hull. The experimental data fitted well to Langmuir and Freundlich isotherms model. The negative values of ΔG^* confirmed a favorable biosorption process at all studied temperatures. The biosorption process is also exothermic in nature. Experimental data were analyzed in terms of pseudo-first order, pseudo-second order and intraparticle diffusion kinetic models. The pseudo-second-order kinetic model was observed to provide the best correlation of the experimental data among the kinetic models studied. To sum up, sunflower seed hull, has a potential to be used as a biosorbent material for the removal of Azure A chloride dye from aqueous solutions because of a bye product of sunflower oil production, its low cost, high biosorption capacity and reasonable rapid rate of biosorption .

REFERENCES

[1]. S. T. Akar,A. Safa Özcan,T. Akara,A. Özcan and Z. KaynakBiosorption of a reactive textile dye from aqueous solutions utilizing an agro-waste. Desalination, 249: 757-761. 2009

[2]. Y. S. Ho, T. H. Chiang, and Y. M. Hsueh, Removal of basic dye from aqueous solution using tree fern as a biosorbent. Process Biochem., 40: 119-124. 2005

[3]. G. McKay, S. J. Allen, I. F. McConvey and M. S. Otterburn. Transport processes in the sorption of colored ions by peat particles. J. Colloid Interface Sci., 80: 323 -339. 1981.

[4]. S. S. Nawar, and H. S. Doma. .Removal of dyes from effluents using low-cost agricultural by-products, Sci. Total Environ., 79: 271-279. 1989.

[5]. R. Gong, Y. Ding, M. .Li, C. Yang, H. Liu and Y. Sun, Y. Utilization of powdered peanut hull as biosorbent for removal of anionic dyes from aqueous solution. Dyes and Pigments, 64: 187-192. 2005.

[6]. A. Witek-Krowiak, R. G. Szafran and S. Modelski. Biosorption of heavy metals from aqueous solutions onto peanut shell as a low-cost biosorbent. Desalination, 265: 126-134. 2011.

[7]. Y. S. Ho, W. T. Chiu and C. C. Wang, Regression analysis for the sorption isotherms of basic dyes on sugarcane dust. Bioresource Technol., 96: 1285-1291. 2007.

[8]. T. Robinson, B. Chandran, and P. Nigam, Removal of dyes from a synthetic textile dye effluent by biosorption on apple pomace and wheat straw, Water Res., 36:2824-2830. 2002.

[9]. X. Wang, L. Xia, K. Tan and W. Zheng. Studies on Adsorption of Uranium (VI) from aqueous solution by wheat straw. Environ. Prog. and Sustain. Energy, 31: 566-576. 2012.

[10]. G. McKay, J, F. Porter and G. R. Prasad, The removal of dye colors from aqueous solutions by adsorption on low-cost materials. Water Air Soil Pollut., 114 : 423-438. 1999.

[11]. A. E. Ofomaja, and Y.S. Ho. Equilibrium sorption of anionic dye from aqueous solution by palm kernel fibre as sorbent. Dyes and Pigments, 74: 60-66. 2007.

[12]. G. Annadurai, R.S. Juang and D.J. Lee Use of cellulose-based wastes for adsorption of dyes from aqueous solutions, J. Hazard. Mater., B92: 263-274. 2002.

[13]. A. Chaparadza and J.M. Hossenlopp. Adsorption kinetics, Isotherms and thermodynamics of atrazine removal using a banana peel based sorbent. Water Science and Technology, 65: 940-947. 2012.

[14]. C. Namasivayam, R, Radhika and S. Suba Uptake of dyes by a promising locally available agricultural solid waste: coir pith. Waste Management., 21 : 38-387. 2001

[15]. R. M. Liversidge, G.J. Lloyd, D.A.J. Wase, and C.F. Forster. Removal of Basic Blue 41 dye from aqueous solution by linseed cake. Process Biochem., 32: 473-477. 1997.

[16]. M. Özacar, and I. A. Şengil, A kinetic study of metal complex dye sorption onto pine sawdust, Process Biochem., 40: 565-572.2005.

[17]. S.P. Raghuvanshi, R, Singh,C. P. Kaushik and A.K. Raghav Removal of textile basic dye from aqueous solutions using sawdust as bio-adsorbent. Int. J. Environ. Stud., 62: 329-339. 2005.

[18]. M.N. Sahmoune, and N. Ouazene. Mass-transfer processes I the adsorption of cationic dye by sawdust. Environ. Prog. and sustain energy, 31: 597- 603.2012.

[19]. W. K. Trotter, H, O. Doty, Jr. W, D. Givan and J. V. Lawler, Potential for Oilseed sunflowers in the United States. US Department of Agriculture Economic Research Service AER 237. 1973.

[20]. National Agricultural Statistics Service (NASS), Acreage report. Agricultural Statistics Board, United States Department of Agriculture (USDA), http://usda01.library.cornell.edu/usda/current/Acre/Acre-06-29-2012.pdf 2012.

[21]. FAO United Nation Food and Agricultural Organization. Major food and Agricultural commodities and producers. FAO. 2011.03.27. 2005.

[22]. North Dakota Agricultural Experiment Station and North Dakota State University Extension Service, Sunflower Production. Extension Publication A-1331,http://www.ag.ndsu.nodak.edu/aginfo/entomology/entupdates/Sunflower/a1331sunflowerhandbook.pdf.2007.

[23]. S. Xu,S, Zhang, K, Chen, J. Han, H, Liu, H. and K. Wu, K. Biosorption of La^{3+} and Ce^{3+} by *Agrobacterium* sp. HN1. J. Rare Earths, 29: 265 -269. 2011

[24]. S.D. Khattri, and M.K. Singh, Use of Sagun sawdust as an adsorbent for the removal of crystal violet dye from simulated wastewater. Environ. Prog, and Sustain. Energy, 31: 435-442. 2012.

[25]. M. S. El-Geundi 1997. Adsorbent for industrial pollution control, Adsorption Science and Technology, 15: 777-787.1997.

[26]. R. G. Sanchez-Duarte, D. I. Sanchez-Machado, J. Lopez-Cervantes, and M.A. Correa-Murrieta, Adsorption of Azure dye by cross-linked chitosan from shrimp waste. Water Science and Technology, 65: 618 -623.

[27]. I. Kiran, T, Akara, A, Safa Ozcanb, A., Ozcanb, and S. Tunali. Biosorption kinetics and isotherm studies of Acid Red 57 by dried Cephalosporium aphidicola cells from aqueous solutions. Biochemical Engineering Journal, 31: 197-203.2006.

[28]. M.V. Subbaiah, Y, Vijaya, A, Subba Reddy, G. Yuvaraja, and A. Krishnaiah, Equilibrium, kinetic and thermodynamic studies on the biosorption of Cu(II) onto Trametes versicolor biomass. Desalination, 276: 310-316. 2011

[29]. S. Ozdemir, F.M. Bekler, V, Okumus, A, Dundar, and E. Kilinc, Bisorption of 2,4-D, 2,4-DP, and 2,4-DB from aqueous solution by using Thermophilic *Anoxybacillus flavithermus* and analysis by high performance thin layer chromatography: Equilibrium and kinetic studies. Environ. Prog. Sustain. Energy, 31: 544-552.2012.

[30]. Malik, P.K., 2004. Dye removal from wastewater using activated carbon developed from sawdust adsorption equilibrium and kinetics. J. Hazard. Mater., 113: 81-88.2004

[31]. N. Kannan, and M.M. Sundaram. Kinetics and mechanism of removal of methylene blue by adsorption on various carbons—a comparative study, Dyes and Pigments, 51: 25-40.2001.

[32]. Y. S. Ho, and G. McKay, Sorption of dye from aqueous solution by peat. Chem. Eng., J. 70: 115-124.1998.

[33]. I. Langmuir, The adsorption of gases on plane surfaces of glass, mica and platinum, J. Am. Chem. Soc., 40: 1361-1403. 1918.

[34]. K. R. Hall, L.C. Eagleton, A, Acrivos and T. Vermeulen, Pore- and solid-diffusion kinetics in fixed-bed adsorption under constant-pattern conditions. Ind. Eng. Chem. Fundam., 5: 212-223 1966

[35]. H.M.F. Freundlich. Uber die adsorption in losungen, Z. Phys. Chem. 57: 385-470. 1906.

[36]. M.M. Dubinin, and L.V. Raduskhevich, The equation of the characteristic curve of the activated charcoal. Proc.Acad.Sci.U.S.S.R Phys.Chem. Sect., 55 : 331.1947.

[37]. F. Helfferich. Ion Exchange, McGrawHill, New York. 1962

[38]. M. S. Onyango,Y, Kojima, O, Aoyi, E,C. Bernardo and H. Matsuda Adsorption equilibrium modeling and solution chemistry dependence of fluoride removal from water by trivalent-cation-exchanged zeolite F-9. J. Colloids Interface Sci., 279: 341-350. 2004

[39]. K. V. Kumar, S. Sivanesan and V. Ramamurthi Adsorption of malachite green onto Pithophora p., a fresh water algae: Equilibrium and kinetic modeling. Process Biochem., 40:2865-2872. 2005

[40]. Wang, B., Hu, Y., Xie, L, .and Peng, K., 2008. Biosorption behavior of azo dye by inactive CMC immobilized Aspergillus fumigatus beads. Bioresource Technol., 99: 794-800. 2008

[41]. T. Akar,A, Safa Ozcan, S, Tunali, and A. Ozcan Biosorption of a textile dye (Acid Blue 40) by cone biomass of Thuja orientalis: Estimation of equilibrium, thermodynamic and kinetic parameters. Bioresource Technology, 99: 3057-3065. 2008

[42]. A. E. Ofomaja, Kinetics and mechanism of methylene blue sorption onto palm kernel fibre. Process Biochemistry, 42: 16-24. 2007.

[43]. M. Aramia,N, Y. Limaeea, N. M. Mahmoodia and N.S. Tabrizia.. Equilibrium and kinetics studies for the adsorption of direct and acid dyes from aqueous solution by soy meal hull. J. of Hazard. Mater., B135: 171-179. 2006.

[44]. J. Gao. J. Wang, C., Yang, S., Wang, and Y. Peng, Binary biosorption of Acid Red 14 and Reactive Red 15 onto acid treated okara: Simultaneous spectrophotometric determination of two dyes using partial least squares regression. Chemical Engineering Journal, 171: 967-975. 2011

Table I. Biosorption Isotherm constants at various temperatures

Temp.(^{o}C)	Freundlich			Langmuir				Dubinin-Radushkevich (D-R)			
	K_F *	n	R^2	K_L **	q_m*	R_L	R^2	q_m	β ***	E ****	R^2
23	2.06	0.82	0.99	0.10	4.61	0.26	0.98	5.83	0.11	2.16	0.93
25	3.38	0.67	0.98	0.14	2.10	0.19	0.97	16.55	0.21	1.55	0.98
30	1.01	1.45	0.97	0.44	3.43	0.08	0.98	1.98	0.02	5.63	0.80
35	1.32	1.68	0.96	0.68	3.45	0.05	0.97	2.51	0.02	5.42	0.84
40	1.10	1.11	0.99	0.04	22.27	0.45	0.99	3.14	0.04	3.68	0.93
45	1.68	0.87	0.87	0.06	9.62	0.37	0.87	5.03	0.08	2.55	0.78

*Unit of K_f and qm: mg g^{-1}

** Unit of K_L : L mg^{-1}

*** Unit of β : mol^2 kJ^{-2}

**** Unit of E : kJ mol^{-1}

Table II. Thermodynamic parameters calculated from the Langmuir constant (K_L) for the Biosorption of Azure dye onto DSSH at various temperatures.

Temp. (°C)	K_L	ΔG^* (kJ mol^{-1})	ΔH^* (kJ mol^{-1})	ΔS^* (J/K mol)
23	0.10	-5.77		
25	0.14	-4.92		
30	0.44	-2.06		
35	0.68	-1.00	-128.50	519.78
40	0.04	-8.23		
45	0.06	-7.48		

Table III. Kinetic parameters for the biosorption of Azure Dye onto DSSH at various dye concentrations

Concentration (mg L^{-1})	k_1 (min^{-1})	q_1 (mg g-1)	R^2	k_2 (g mg^{-1}min^{-1})	q_2 (mg g^{-1})	R^2	K_{id} (mg g^{-1}min$^{-0.5}$)	R^2
11.70	0.008±0.0003	2.37±0.02	0.79	0.06±0.001	1.10±0.02	0.99	0.06	0.99
15.21	0.015±0.0009	1.41±0.06	0.89	0.045±0.002	1.46±0.01	0.99	0.14	0.99
17.85	0.016±0.0007	1.24±0.06	0.90	0.043±0.004	1.70±0.00	0.99	0.13	0.99
23.65	0.016±0.0008	1.08±0.04	0.90	0.03±0.001	2.26±0.01	0.99	0.19	0.99
28.50	0.018±0.0009	1.47±0.08	0.94	0.02±0.001	2.70±0.01	0.99	0.24	1.00
31.00	0.008±0.0003	1.13±0.02	0.83	0.02±0.001	2.88±0.03	0.99	0.16	0.99

Fig. 1: Chemical structure of Azure Chloride A dye

Fig.2: Effect of pretreatment on biosorption capacity of DSSH

Fig. 3: Effect of particle size on biosorption capacity of DSSH

Fig 4: Effect of time on bisorption of Azure Dye on DSSH

Fig. 5: Effect of pH on % dye biosorbed (PDB) (□) and biosorption capacity (◊) of DSSH.

Fig. 6: Effect of dye concentration on percent dye biosorbed PDB (◊) and biosorption capacity (□)

Fig. 7: Effect of biosorbent dosage on the PDB(□)and biosorption capacity (◊) at room temperature.

Fig. 8: Langmuir isotherm plots for the biosorption of Azure dye by DSSH at different temperatures.. (ж)
23°C (Δ) 25°C; (◊) 30°C ; (□) 35°C;(X) 40°C;; (O) 45°C

Fig. 9: Freundlich isotherm plots for the biosorption of Azure dye by DSSH at diifferent temperatures. (ж)
23°C (Δ) 25°C; (◊) 30°C ; (□) 35°C;(X) 40°C;; (O) 45°C

Fig. 10: D–R isotherm plots for the biosorption of Azure dye by DSSH at different temperatures.
(*) 23°C (Δ) 25°C; ($\Diamond$) 30°C ; ($\Box$) 35°C;(X) 40°C;; (O) 45°C

$$y = -15456x + 49.93$$
$$R^2 = 0.963$$
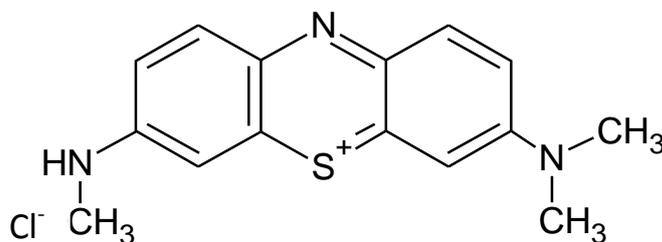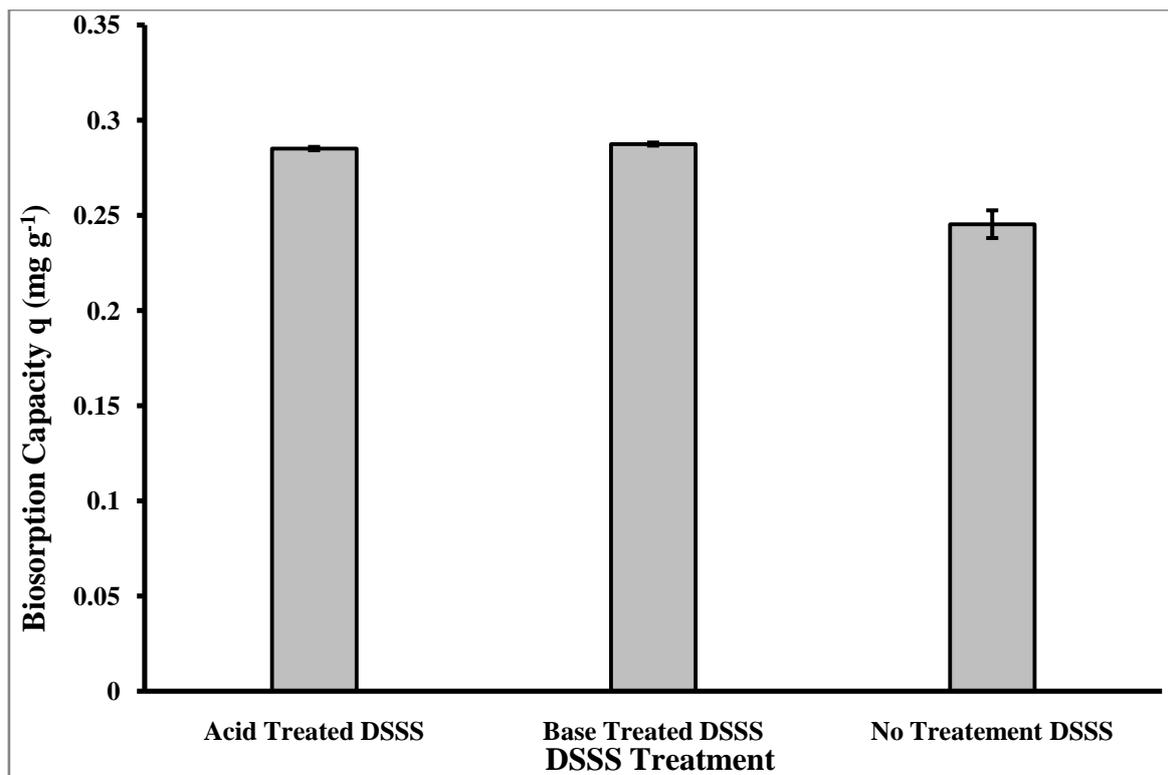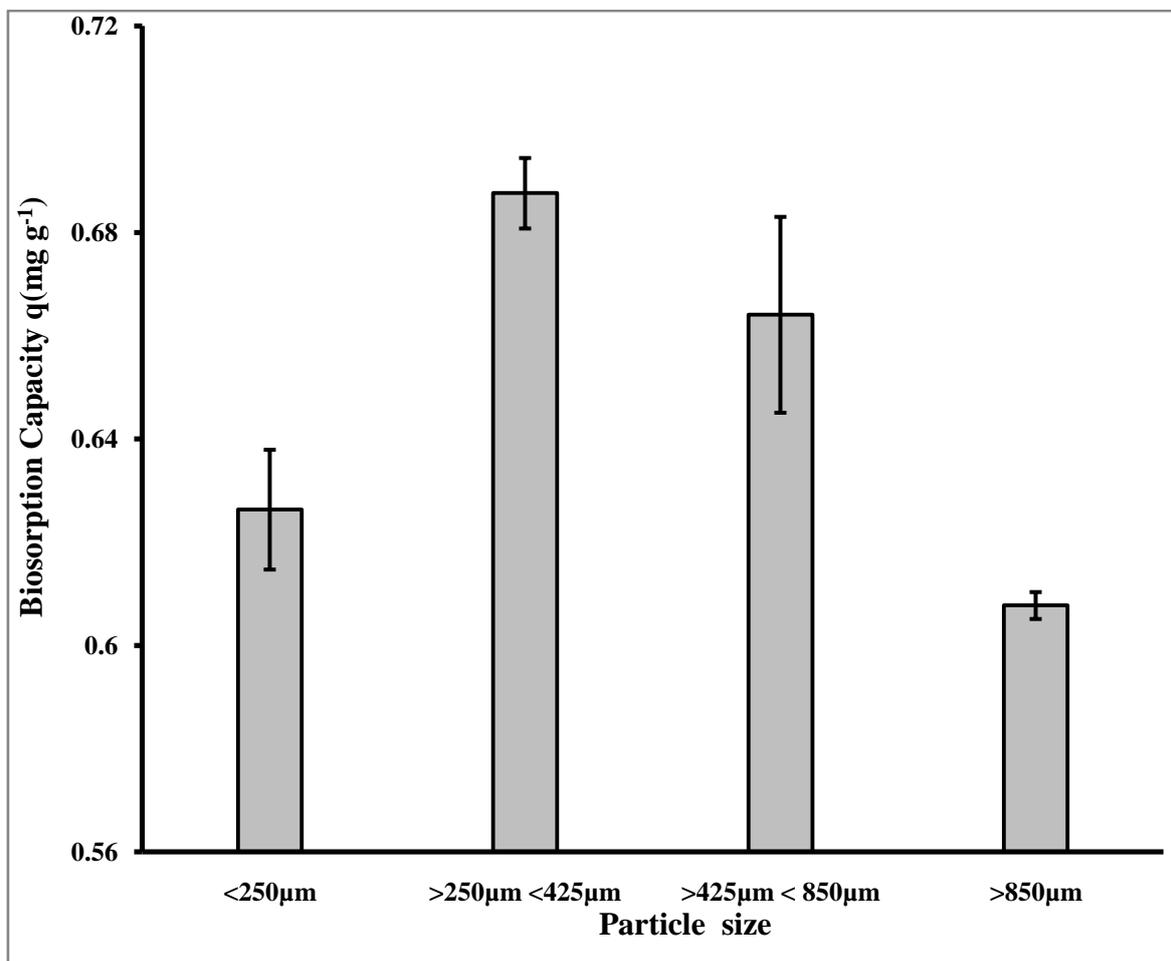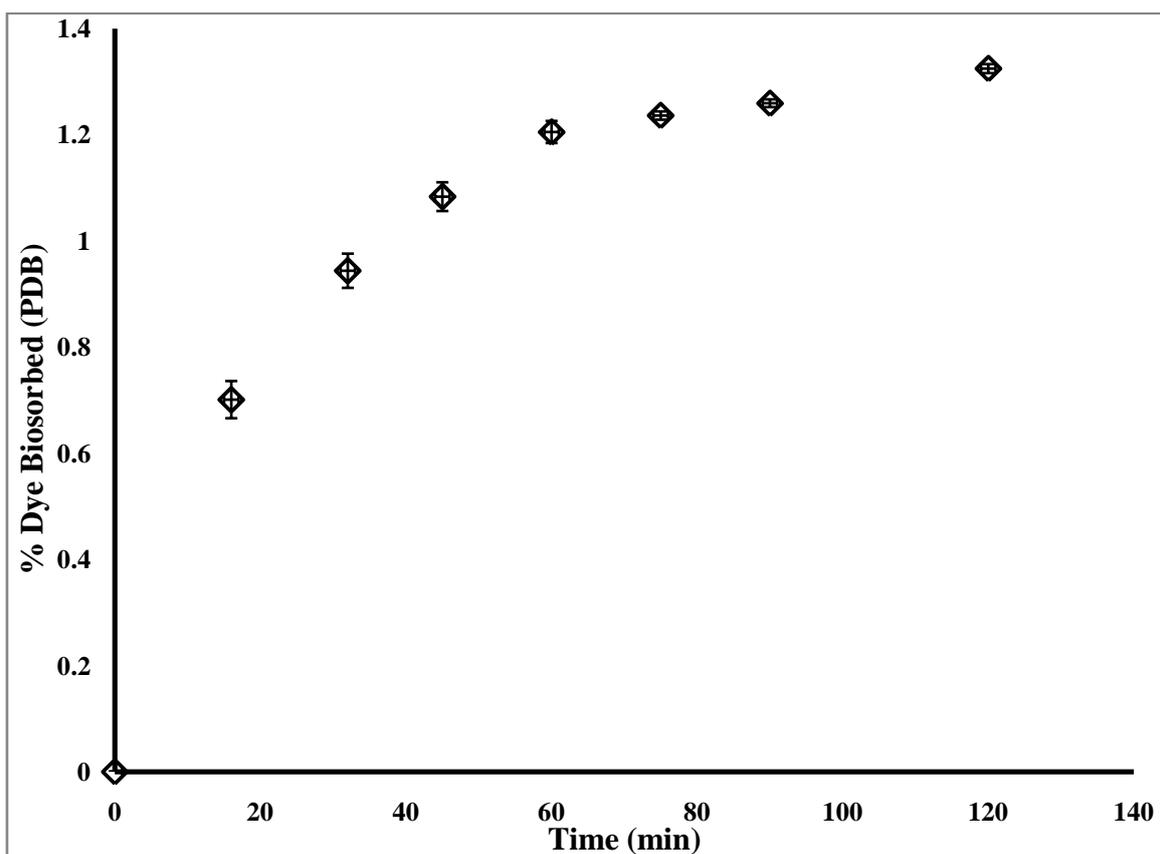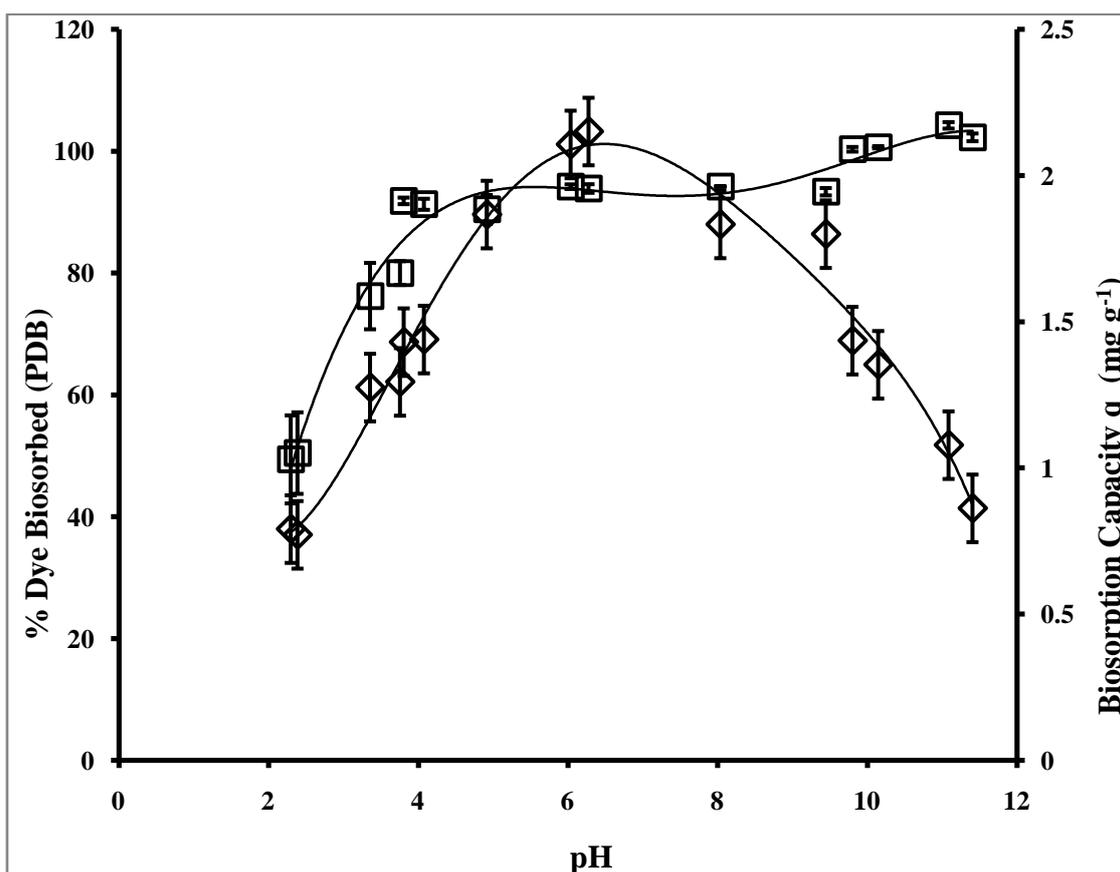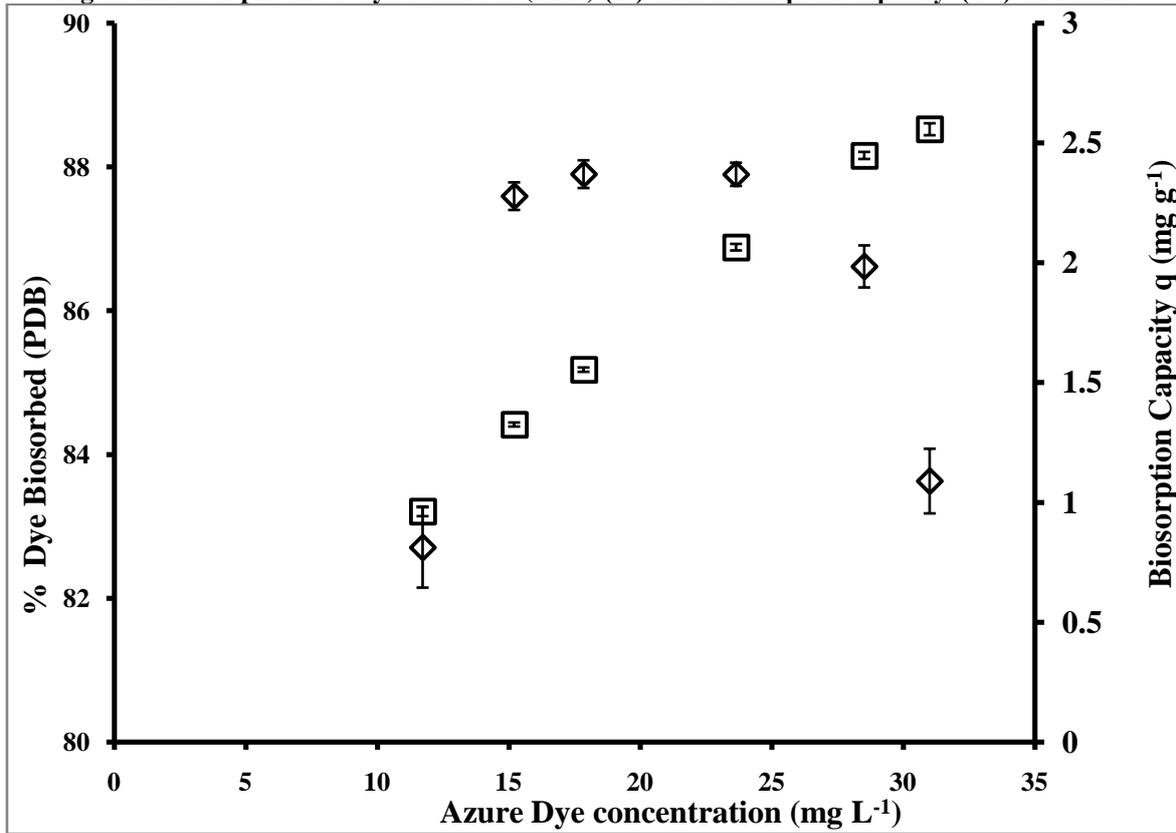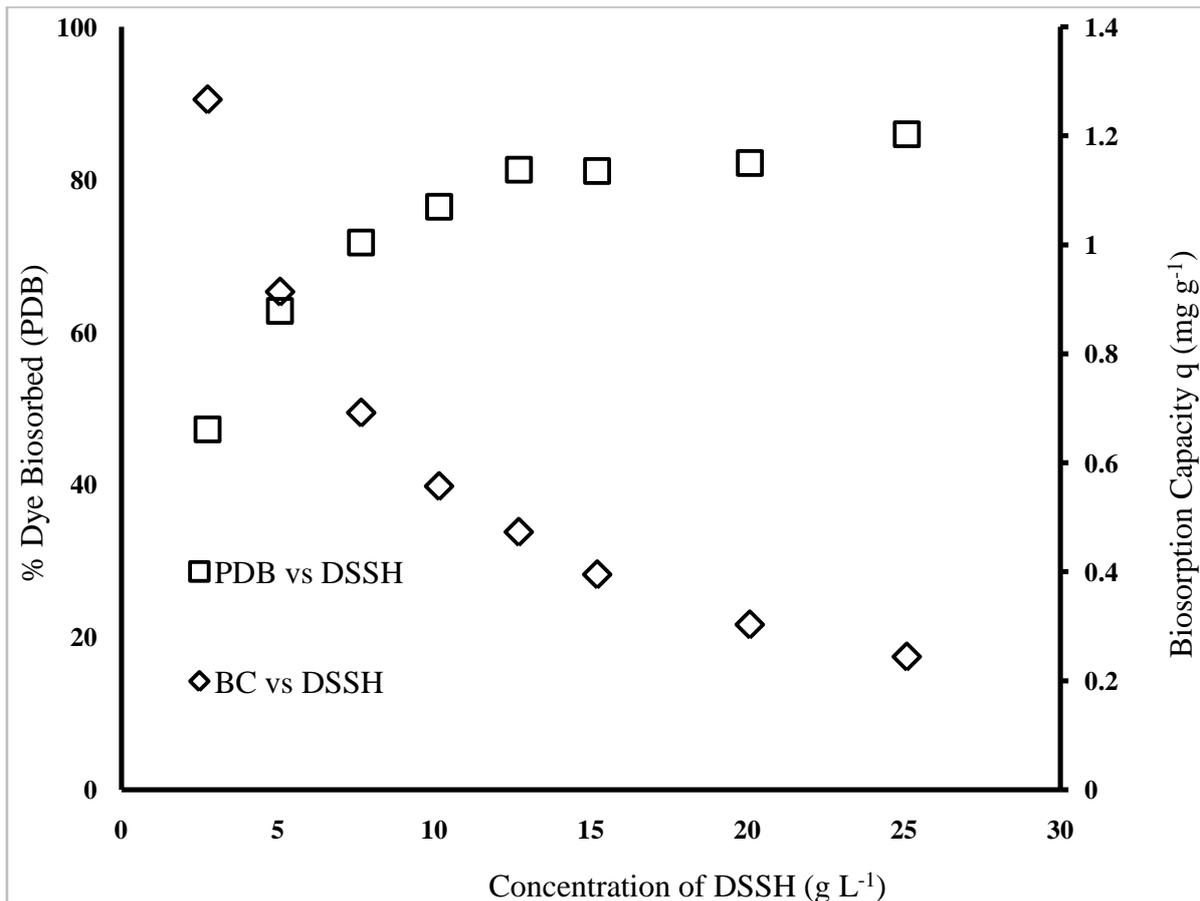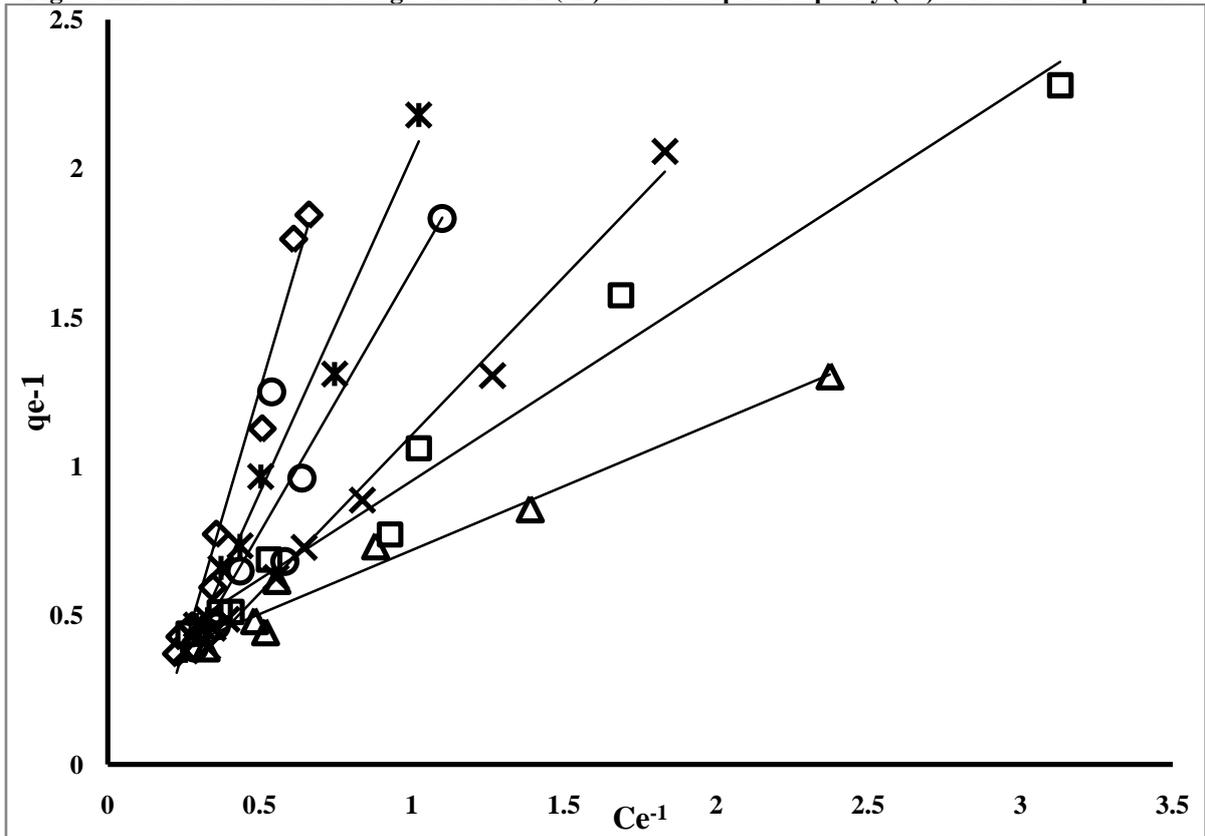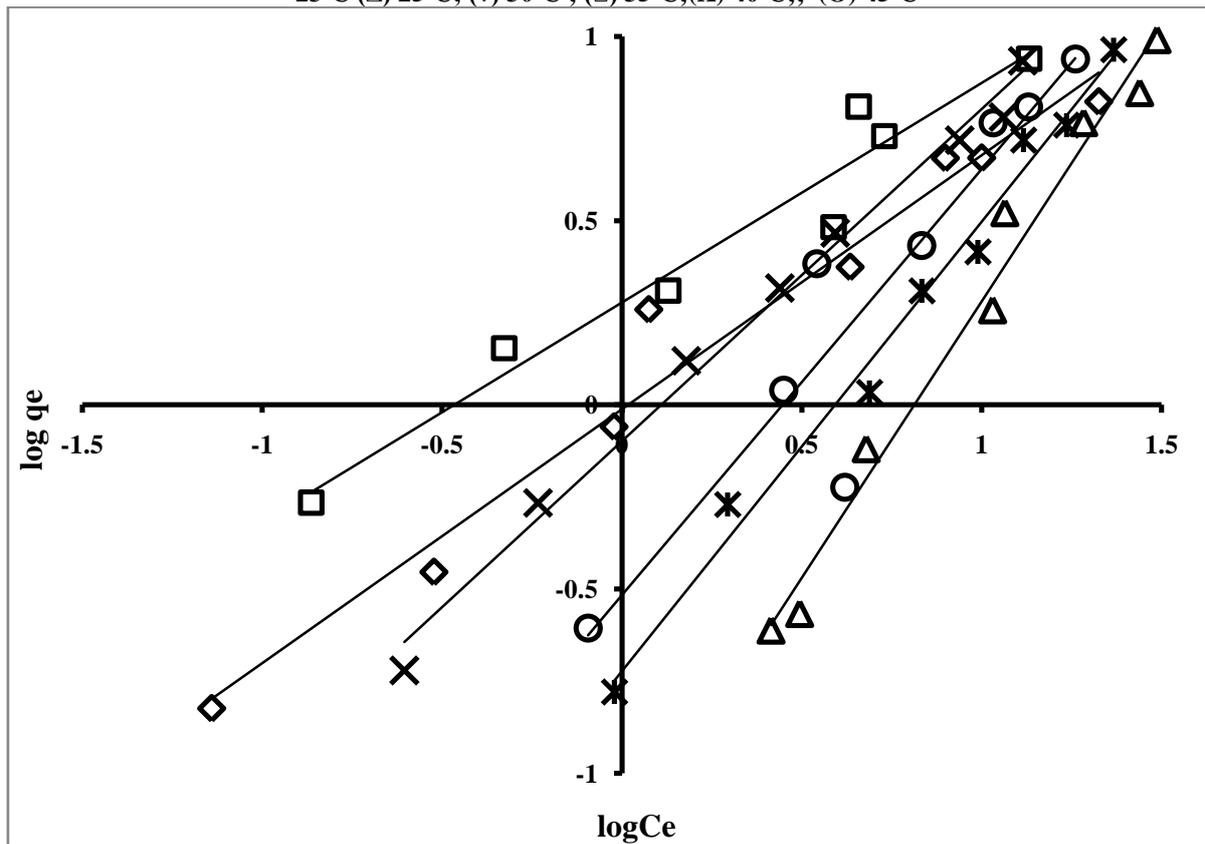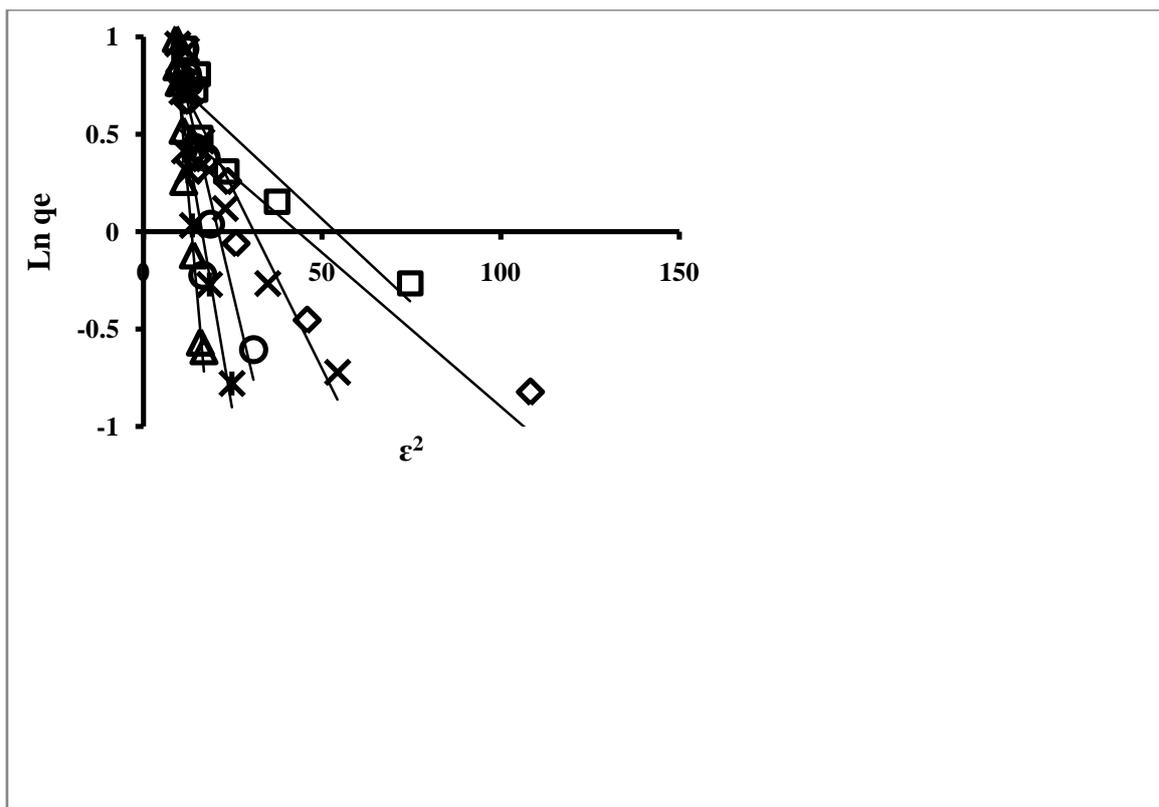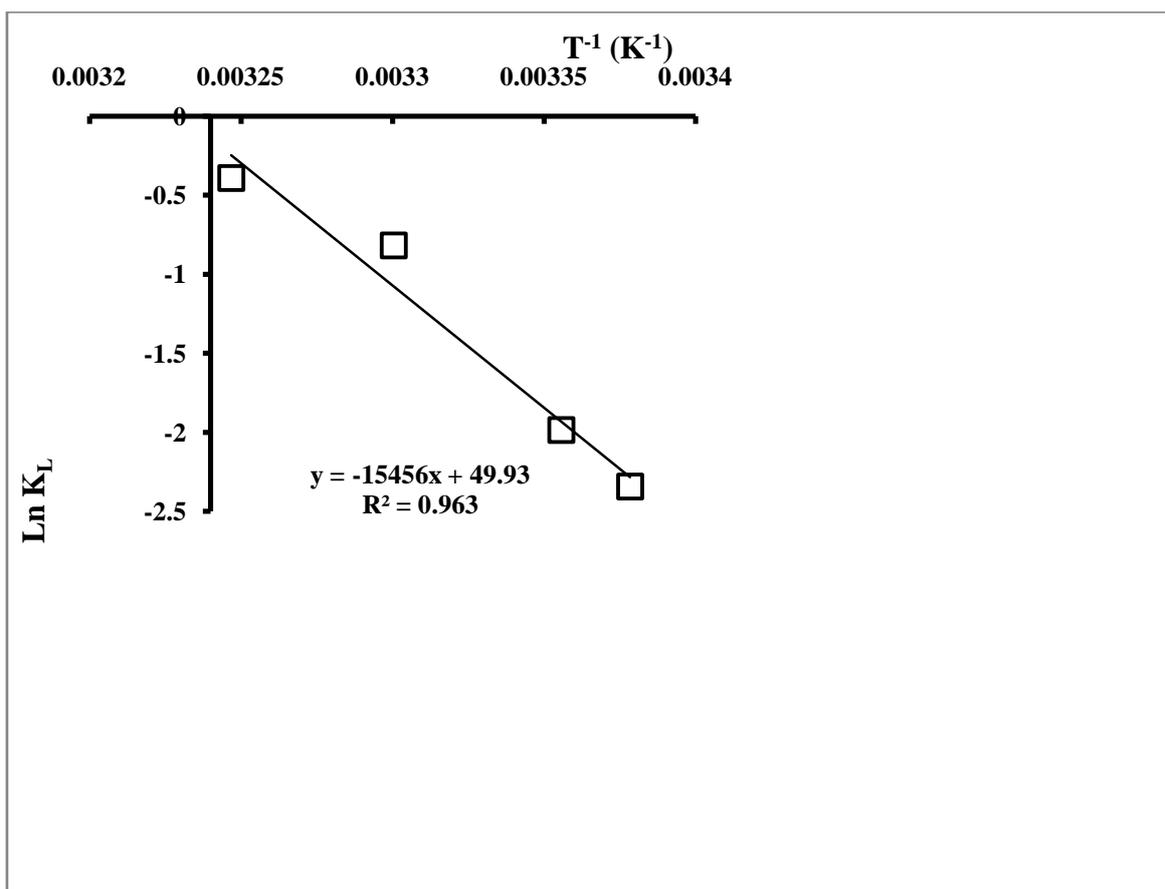
Fig. 11: Plot of Ln K$_L$ versus T^{-1} for estimation of thermodynamic parameters

for the biosorption of Azure dye onto DSSH.
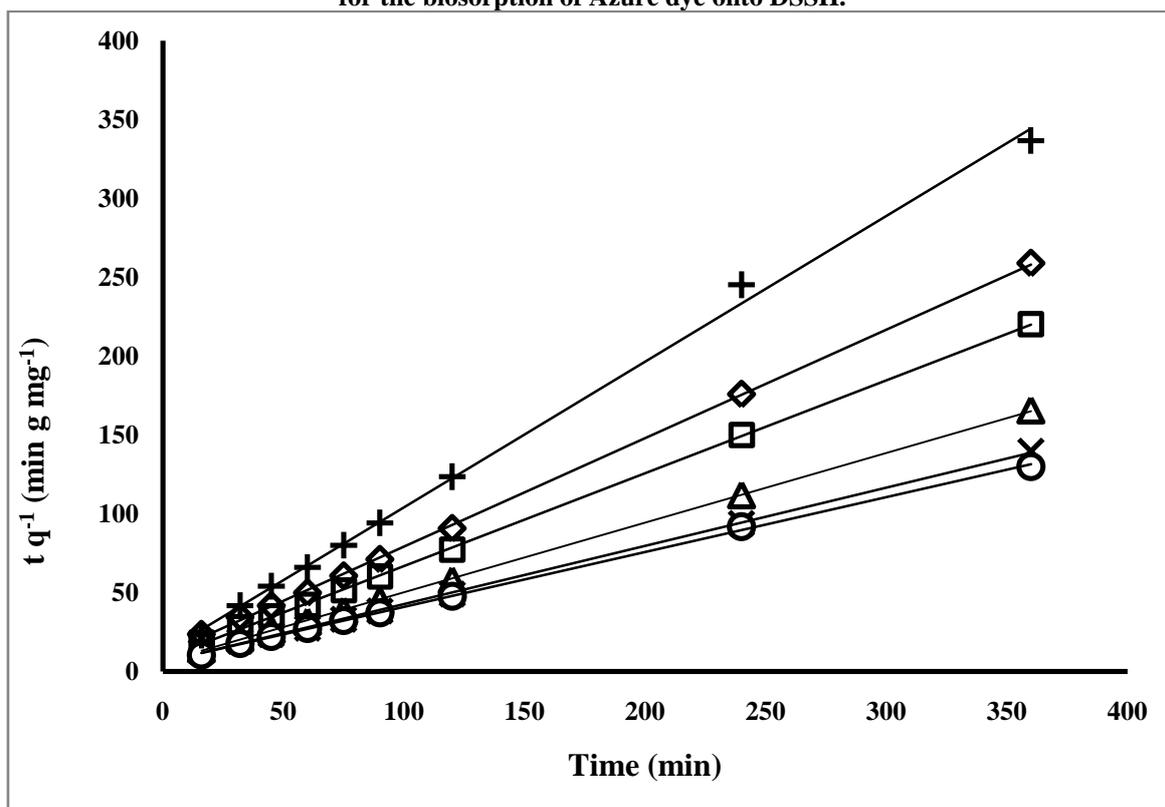
Fig.12: Pseudo-second-order kinetic plots for the biosorption of various Azure dye concentrations (+) 11.7 mg L^{-1}; (◊) 15. 21 g mL^{-1}; (□) 17.85 mg L^{-1};(Δ) 23.05 mg L^{-1}; (X) 28.5 mg L^{-1} ; (O)31.75mg L^{-1} onto DSSH
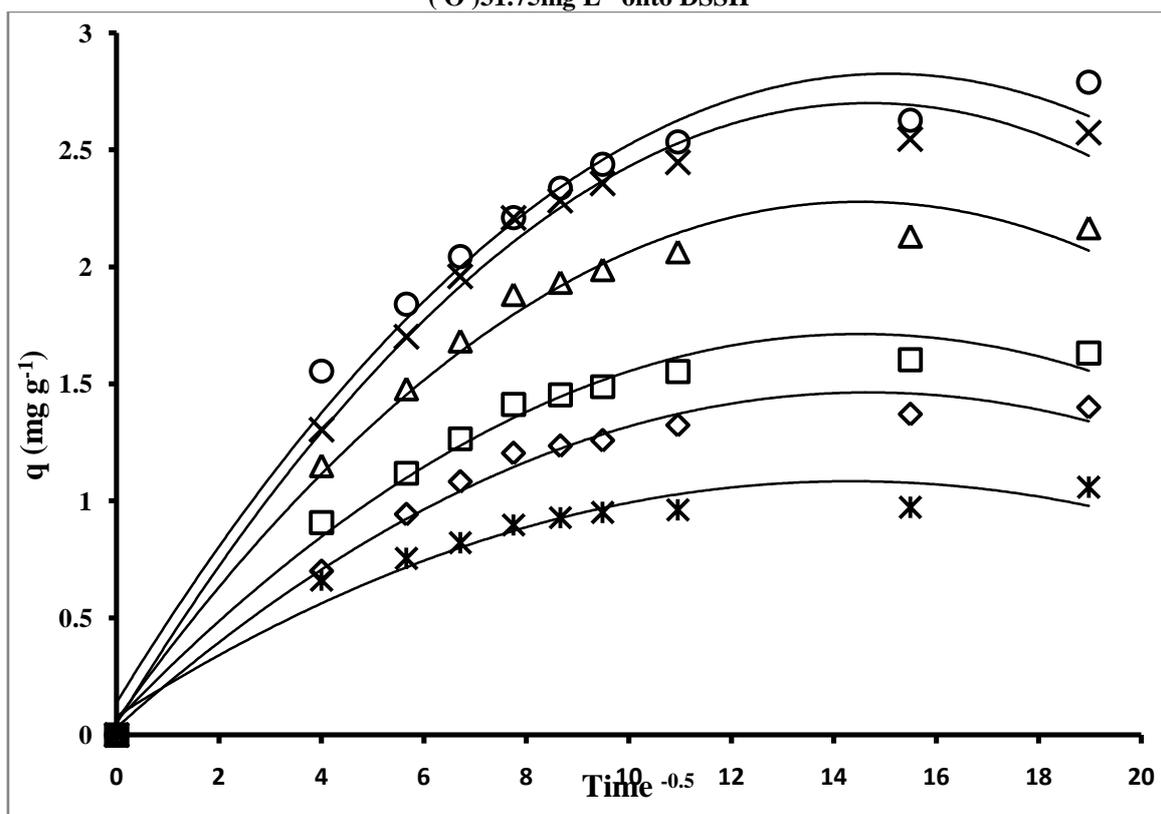
Fug. 13: Intraparticle diffusion kinetic model plots for the biosorption of various Azure dye concentrations (*) 11.7 mg/L; (Δ) 15. 21 g/L; (□) 17.85 mg/L;(◊) 23.05 mg/L; (X) 28.5 mg/L ; (O)31.75mg/L onto DSSH